J Mater Sci: Mater Electron (2017) 28:12458–12466
DOI 10.1007/s10854-017-7067-3

Effects of annealing temperature on the structural, morphology, optical properties and resistivity of sputtered CCTO thin film

Mohsen Ahmadipour[1] · Mohd Fadzil Ain[2] · Zainal Arifin Ahmad[1]

Received: 30 December 2016 / Accepted: 2 May 2017 / Published online: 9 May 2017

Abstract $CaCu_3Ti_4O_{12}$ (CCTO) thin films with a thickness of 200 nm were deposited on ITO substrates by RF magnetron sputtering using a pure CCTO target. After the deposition, thin films were annealed at 400, 450, 500 and 550 °C, respectively, for 1 h. The effects of annealing temperature on the structural, surface morphology, optical properties and resistivity of (CCTO) thin films were investigated. The X-ray diffractometer results show that the thin films are polycrystalline in nature and are assigned to body-centered cubic perovskite configuration with a space group of Im-3. The intensity of the peaks and crystallinity gradually increased with the increase in annealing temperature. Microstructural investigation through FESEM showed that the grain size increased with increase in annealing temperature from 32 to 85 nm. The root mean square and roughness (Ra) were also enhanced with higher annealing temperatures, from 3.8 to 6.2 nm and from 4.7 to 7.7 nm, respectively, as confirmed by AFM. Increase in annealing temperature also affected the optical transmittance values which decreased to almost 60% at the visible range (550–850), as well as the optical energy band gap which decreased from 3.86 to 3.39 eV. The relevance between resistance behaviors and film microstructure is discussed. Therefore, it can be concluded that the desirable crystallinity, surface roughness, energy band gap and resistivity for 200 nm thick CCTO thin films deposited by RF magnetron sputtering can be achieved through the annealing process.

✉ Zainal Arifin Ahmad
srzainal@usm.my

[1] Structural Materials Niche Area, School of Materials and Mineral Resources Engineering, Universiti Sains Malaysia, Engineering Campus, 14300 Nibong Tebal, Penang, Malaysia

[2] School of Electrical and Electronic Engineering, Universiti Sains Malaysia, Engineering Campus, 14300 Nibong Tebal, Penang, Malaysia

1 Introduction

Materials with high dielectric permittivity (ε_r) have received considerable attention due to their extensive use in technological applications. Today, among the many inorganic materials, CCTO is considered versatile and is widely used in many areas of application such as capacitors [1], microwave devices and antennas [2], and humidity sensors [3, 4] due to its high ε_r, moderate dielectric loss (tanδ) [5], high electrochemical and thermal stability [6], and wide direct band gap [7]. A number of top-down and bottom-up approaches such as RF magnetron sputtering, pulsed laser deposition, metal organic chemical vapor deposition (MOCVD), and sol–gel deposition [8–12] have been used to deposit CCTO thin films.

Among these methods, RF magnetron sputtering is a cost-effective technique for the deposition of the film over a large area, has better coating uniformity, and offers more freedom in selection of deposition conditions; these are properties that are of great interest for different applications. There are only a few reports on the fabrication of CCTO thin films using RF magnetron sputtering process for the investigation of its gas-sensing properties and ε_r. For example, Joanni et al. [7] reported the gas-sensing properties of CCTO thin films deposited on Si/SiO_2/Ti/Pt substrates by RF magnetron sputtering; the response time and sensitivity of the gas sensor (O_2) was reported to be 5 min and 2.6, respectively. On the other hand, the ε_r of CCTO thin films deposited on Pt(111)/Ti/SiO_2/Si was reported to be ~5000 at 1 kHz by Prakash et al. [13]. However, both of these CCTO thin films did

not go through the annealing process. The annealing process is expected to be a very effective method in changing and enhancing the structural and physical properties of the films prior to the fabrication of any devices such as sensors, capacitors, antennas, non-linear optical devices, microwave devices, and resistive switches. Since the microstructure of the thin film consists of small crystals/grains which act as one of the most effective factors, it will determine the overall mechanical, optical, and electrical behavior of the film. For example, finer crystals/grains (<100 nm) deliver a more sensitive electrical response which is useful for sensor applications. Heat treatment processes such as annealing provides an efficient way to manipulate the properties of materials by controlling the diffusion and cooling rates within the microstructure.

In this paper, the effects of annealing temperature on the structural and optical properties, surface morphology, and resistivity of CCTO thin films were investigated at various temperatures (400, 450, 500 and 550 °C). The 200 nm thick CCTO thin films used in this work were deposited on ITO substrate by RF magnetron sputtering using a pure CCTO target.

2 Experimental procedure

CCTO thin films with a thickness of 200 nm were deposited on ITO substrates (3×3 cm^2) by RF magnetron sputtering (HHV Auto 500). The film was deposited at 1.23×10^{-2} mbar sputtering pressure, 10 sccm argon gas flow rate, and 150 W of RF power. The base pressure in the chamber was evacuated to 30×10^{-5} mbar using a turbo molecular pump. A CCTO target (99.99% purity) with a diameter of 76.2 mm and thickness of 5 mm (Semi-conductor Wafer, Inc., Taiwan) was used. The ITO substrates (1.1 mm thickness) were purchased from Magna Value Sdn. Bhd. Malaysia. The arrangement of the sputtering process is shown in Fig. 1. The ITO substrate was fixed on the rotatable and heatable disk holders. During deposition, the substrate was heated at 300 °C and rotated to improve film uniformity. The target was pre-sputtered for 10 min to clean the target surface. Before the deposition, the substrates were ultrasonically cleaned in acetone and then ethanol for 30 min to remove surface impurities after which they were dried with flowing oxygen. After deposition, the CCTO films were subjected to the annealing process in a furnace (KHT-1600X) with atmospheric environment of 400, 450,

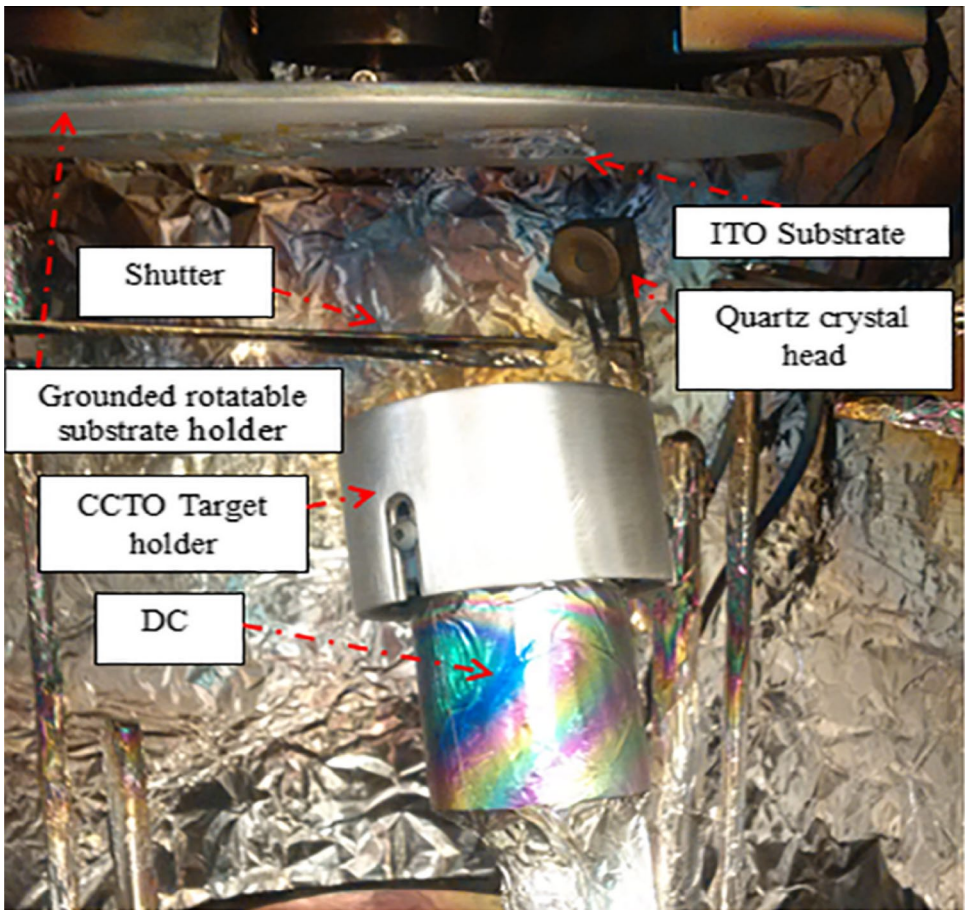

Fig. 1 RF magnetron sputtering system

500, and 550 °C for 1 h, respectively. The details for the sputtering conditions are shown in Table 1.

The deposited CCTO films were examined by an X-ray diffractometer (XRD, D8Advance, Bruker) with Cu Kα radiation together with Highscore Plus software (PANAlytical). The morphology of the films was investigated using a field emission scanning electron microscope (FESEM, Zeiss Supra™ 35VP) while the surface morphology was analyzed by atomic force microscope (AFM, Nano Navi, SPA 400). Optical transmittance measurements were performed with a UV–Vis spectrophotometer (Varian, Cary 50 conc) at the wavelength range of 270–900 nm. The resistance behavior of the CCTO thin films was measured using a Keithley electrometer (Model 2611A).

Table 1 Experimental parameters of the deposition process using RF magnetron sputtering system

Parameter	Unit	Value
Vacuum pressure	mbar	2×10^{-5}
Operation pressure	mbar	1.23×10^{-2}
Base pressure	mbar	30×10^{-5}
Power	watt	150
Deposition time	min	120
Distance	mm	120
Sputtering gas		Ar
Gas temperature	pa	Room temperature
Gas flow rate	sccm	10
Substrate temperature	°C	300
Film thickness	nm	200

3 Results and discussion

Figure 2 shows the XRD patterns of CCTO thin films as-deposited and after-annealing at different temperatures (400, 450, 500, and 550 °C, respectively). These XRD patterns can be assigned to $CaCu_3Ti_4O_{12}$ body-centered cubic perovskite related structures (ICDD data card no. 98-005-8088) with a space group of Im-3. The films were less crystalline at lower annealing temperatures due to defects, grain mobility caused by reorientation towards their respective planes, and a lack of sufficient kinetic energy. The CCTO thin films' degree of crystallinity was found to increase with increase in temperature as shown by the increasing intensity of (112), (022), (033) and (224) peaks with increasing annealing temperature. The degree of crystallinity of the sample can also be determined from XRD deconvolution. The degree of crystallinity, *Xc*, can be calculated using Eq. (1) [15].

$$\mathrm{Xc}(\%) = \frac{\mathrm{A_c}}{\mathrm{A_c} + \mathrm{A_a}} \times 100\% \quad (1)$$

Here, A_c is the area under the peaks, representing the total crystalline region, and A_a is the area under the peaks, representing the total amorphous region. The value of

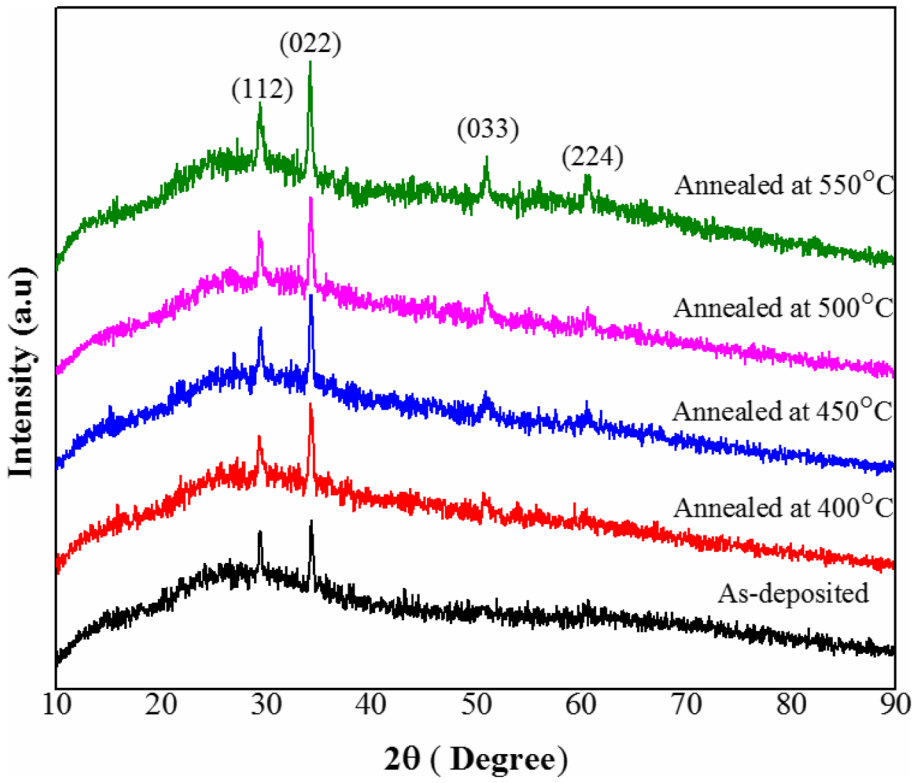

Fig. 2 Typical XRD patterns for as-deposited CCTO thin films and for CCTO films annealed at *four* different temperatures

crystallinity are 48.4, 50.3, 56.7, and 59.8% for CCTO thin films annealed at 400, 450, 500, and 550 °C, respectively.

Figure 2 also shows the enhancement of peaks according to temperature. This observation can be further confirmed through its crystallite size (D) calculation using Debye–Scherrer's formula (Eq. 2) [16]:

$$D = \frac{K\lambda}{\beta \operatorname{Cos} \theta} \tag{2}$$

where D is the crystallite size, K is the constant equals to 0.9, λ is the wavelength of Cu Kα radiation (λ = 1.54060°A), β is FWHM, and θ is the Bragg's angle.

D was calculated from the full width at half maximum (FWHM) of CCTO's sharpest peak (022) as a function of temperature, as given in Table 2. The XRD analysis shows that the D values corresponding to the (022) plane increased with increasing annealing temperature; this illustrates enhancement in crystallinity [17].

Figure 3 shows FESEM micrographs of the CCTO thin films. The thickness of the films is clearly shown as 200 nm (Fig. 3a). Figure 3b–f shows the morphological changes of the CCTO thin films before and after being annealed at different temperatures (400, 450, 500 and 550 °C). Morphology is among the important factors responsible for the physical and electrical properties of the film. The average grain size of CCTO before annealing was about 32 nm (Fig. 3a) and was gradually increased to 43 nm (annealed at 400 °C); it finally became 85 nm at 550 °C. The annealed CCTO films showed a smooth, compact, and densely packed morphology. The growth of the grain size can be attributed to the fact that the CCTO thin films experienced change in grain boundary at the specific annealing temperatures [18]. In addition, with the increase in annealing temperature, these small grains coalesce together to form larger grains (Fig. 3e). This process of coalescence also causes major grain growth in surface roughness. With further increment in annealing temperature, larger grains start to develop due to aggregation and interconnection of small grains (Fig. 3f). Therefore, it can be concluded that CCTO thin films' grain size increases with the increase in annealing temperature, as corroborated by AFM measurements. This indicates that the morphology and grain size of the CCTO thin films can easily be modified through the annealing process.

The chemical compositions of CCTO thin films annealed at different temperatures were obtained quantitatively from EDAX (Table 2). As shown in Table 2, the atomic percentage of substrates Si and Ca, Cu, Ti, and O remained almost the same.

A further detailed analysis on the CCTO thin films' surface morphology can be done using the AFM technique. Figure 4 shows AFM micrographs of the CCTO thin films using tapping mode at ambient condition. It can be clearly

Table 2 Data evaluated from the XRD, FESEM, EDAX, AFM and UV–Vis measurements of CCTO thin films after annealing at different temperatures

Annealing temperature (°C)	2θ (022) (°)	FWHM (022) (°)	Crystallite size (022) (nm)	Average grain size (nm) (FESEM)	Atomic (%)					Roughness (Ra)	Root mean square (RMS)	Optical band gap (eV)
					Si	Ca	Cu	Ti	O			
As-deposited	35.680	0.270	30 ± 0.16	32	24.08	3.83	11.28	15.19	45.62	3.80 ± 0.12	4.76 ± 0.12	3.86
400	35.701	0.267	31 ± 0.16	43	23.87	3.82	12.09	15.01	45.21	3.87 ± 0.12	4.98 ± 0.10	3.80
450	35.720	0.234	35 ± 0.13	56	23.59	3.78	12.15	15.12	45.36	4.70 ± 0.12	6.03 ± 0.10	3.70
500	37.781	0.230	36 ± 0.15	61	20.70	3.99	12.39	15.77	47.15	4.84 ± 0.11	6.09 ± 0.11	3.64
550	35.785	0.219	39 ± 0.16	85	21.03	4.02	12.20	15.58	47.17	6.28 ± 0.12	7.70 ± 0.10	3.39

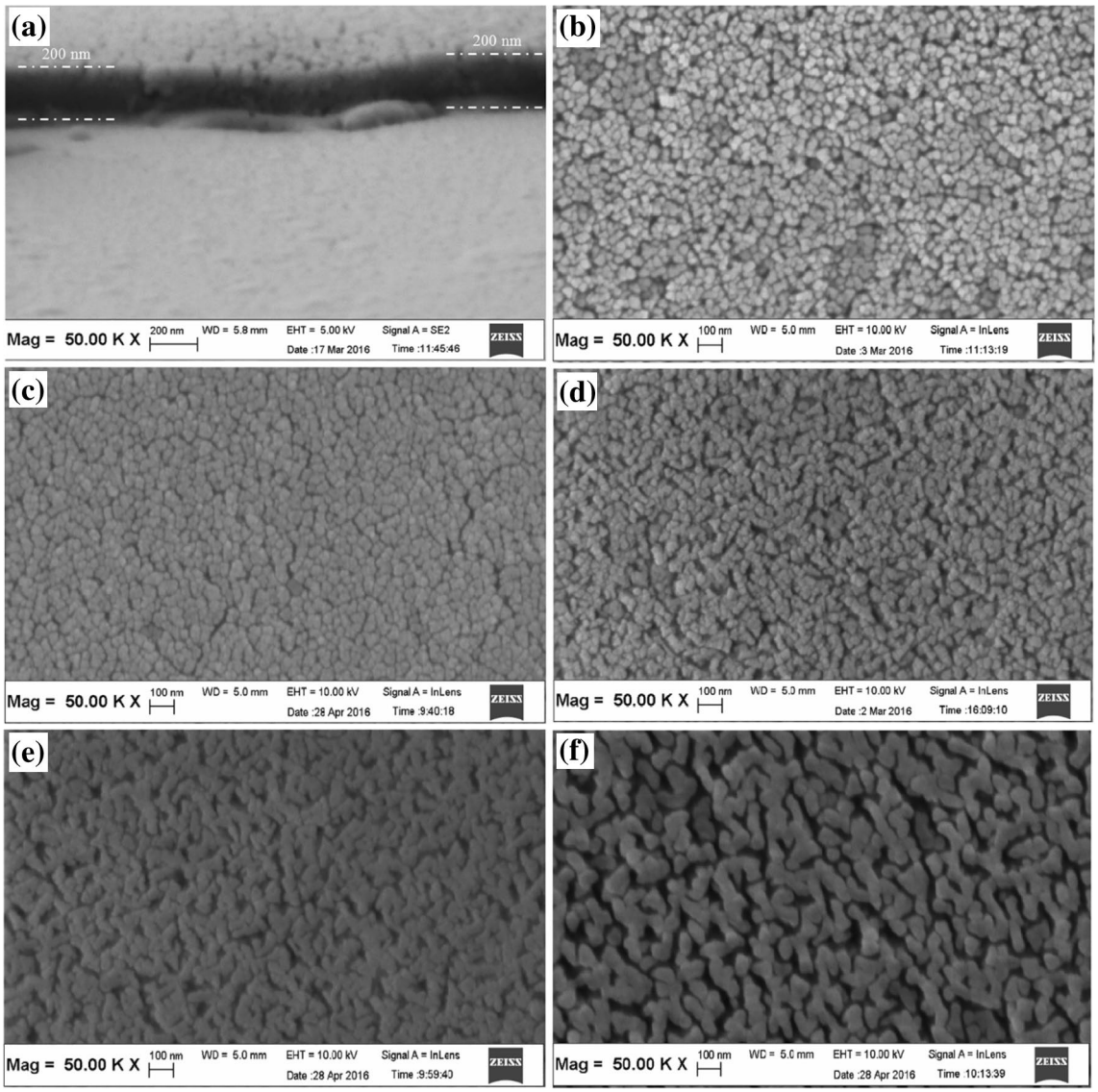

Fig. 3 FESEM micrographs for CCTO thin films annealed at **a** as-deposited, **b** 400 °C, **c** 450 °C, **d** 500 °C, **e** 550 °C, and **f** cross-section image of CCTO thin film

seen that different annealing temperatures have obvious effects on the surface roughness. The CCTO thin films exhibited microstructures consisting of small and large grains. The roughness (Ra) and root mean square (RMS) of the roughness were determined by the AFM from the scan area of 10×10 μm^2 with the help of Nano Navisoftware for imaging; the values were found to have increased with increasing annealing temperature. This can be explained in terms of major grain growth which yields an increase in the surface roughness [19].

To verify the importance of the annealing process on the CCTO thin films, changes in optical property in relation to annealing temperature was observed, as shown in Fig. 5. The measurements of optical properties of the films annealed at 400, 450, 500, and 550 °C were taken in the range of 270–900 nm under ambient condition (Fig. 5a). It was revealed that the transmittance was reduced to almost 60% at the visible range (550–850) with increasing annealing temperature. Therefore, the main cause for the decrease in transmittance can be inferred to be due to the reflected light and rough surfaces scattered, as surface roughness (Fig. 4) increased due to higher annealing temperatures. Another optical property that can be obtained from this measurement is the energy band gap. The values were estimated by employing the Tauc plot model (Eq. 3) [20]:

$$(\alpha h\nu)^2 = C\left(h\nu - E_g\right) \tag{3}$$

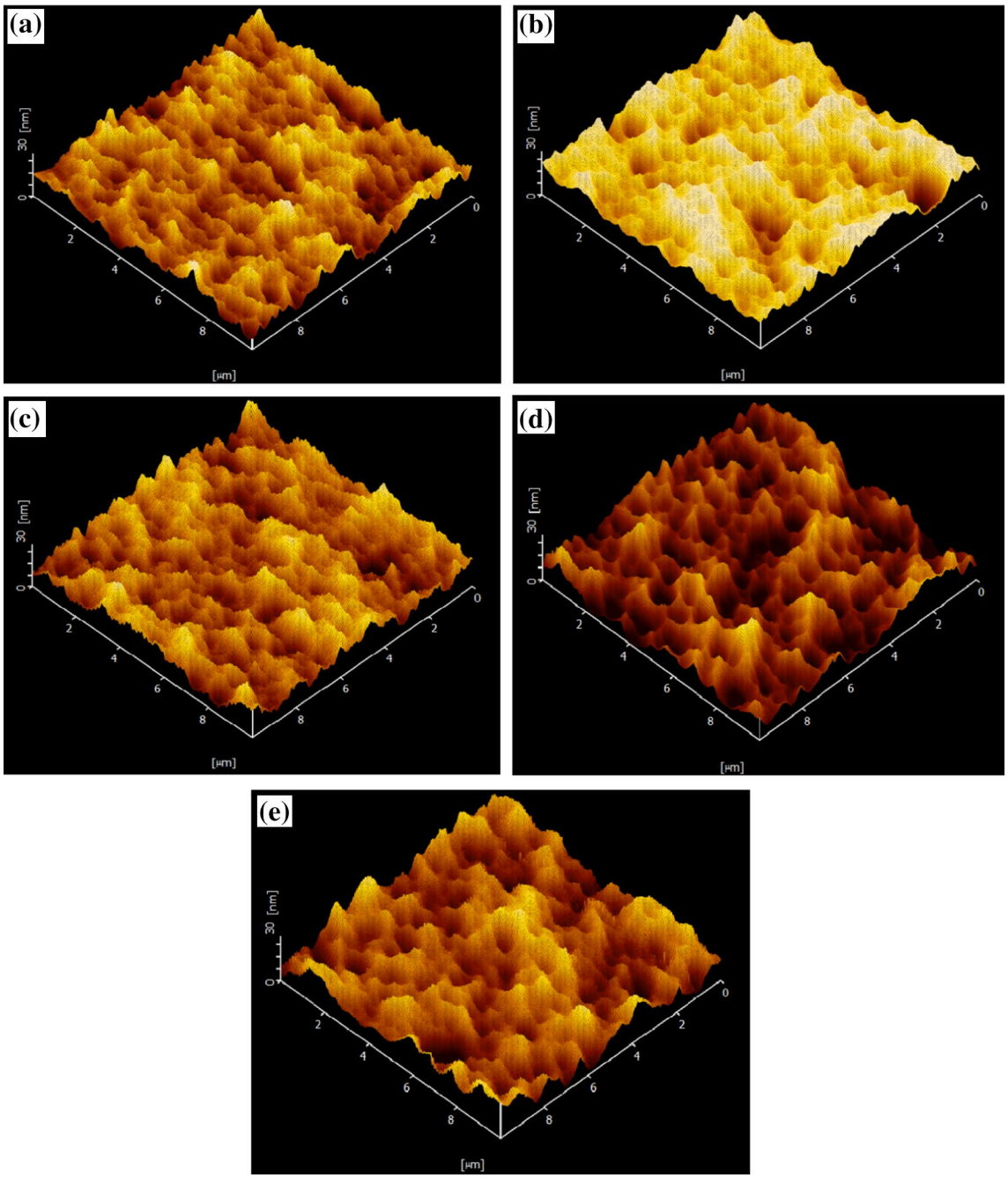

Fig. 4 AFM images of CCTO film annealed at different temperatures **a** as-deposited, **b** 400 °C, **c** 450 °C, **d** 500 °C, and **e** 550 °C

where α is the absorption coefficient, hν is the photon energy, C is a constant (velocity of light), and E_g is the energy band gap.

The E_g values of the films annealed at different temperatures were determined by the extrapolation of the straight section to the energy axis of the plot i.e. $(\alpha h\nu)^2$ versus photon energy (Fig. 6b). The E_g values of the films show a decrease in energy band gap with increased annealing temperature. The shift of E_g can be attributed to the effect of increased grain size with increasing annealing temperatures [21]. The E_g of 200 nm thick CCTO thin films decreased with increasing annealing temperatures, from 400 to 550 °C, reaching a minimum of 3.39 eV at 550 °C. The E_g values of the CCTO thin films were determined as 3.86, 3.8, 3.7, 3.64, and 3.39 for as-deposited, 400, 450, 500, and 550 °C annealed samples, respectively.

To date, no investigations on the effects of annealing temperature on optical properties of CCTO thin

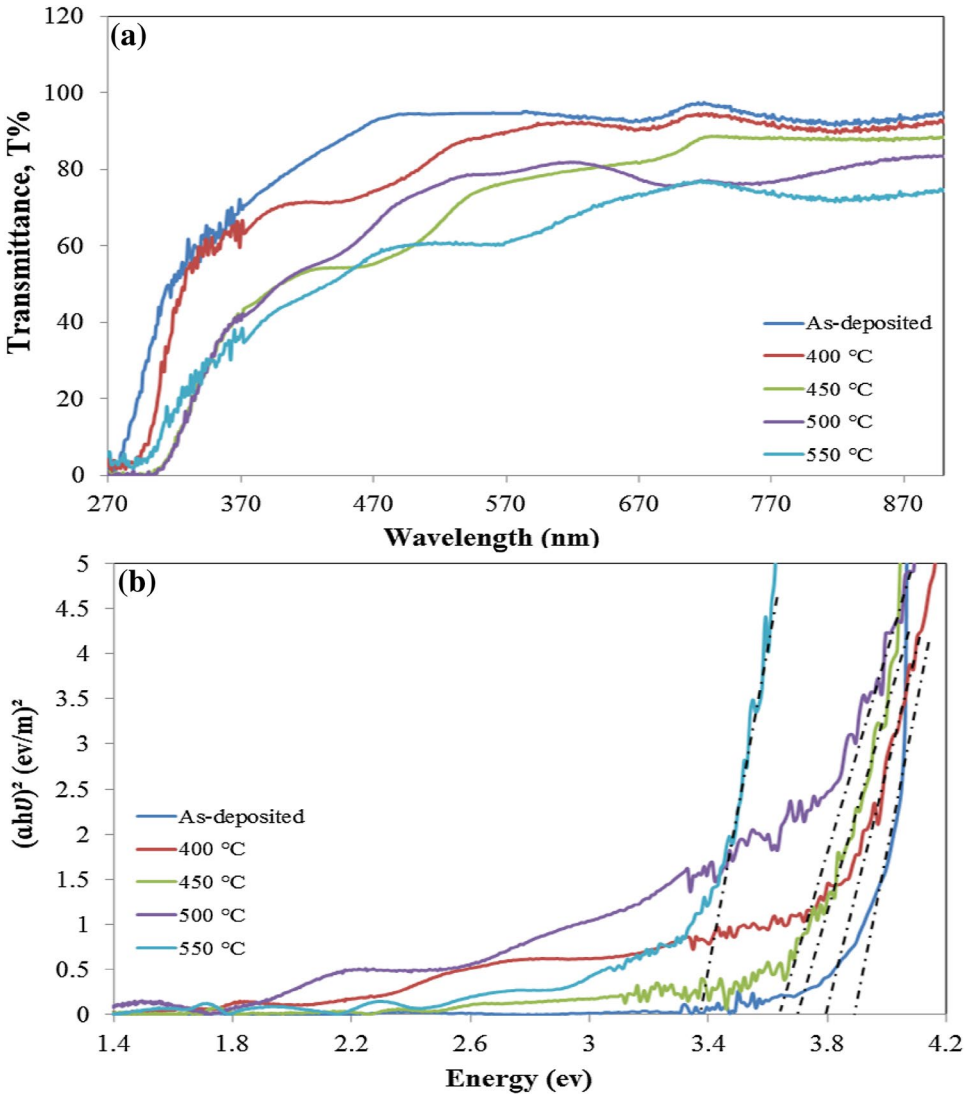

Fig. 5 **a** Optical transmittance spectra and **b** energy band gap of CCTO film before and after annealing

films have been reported. Turky et al. [22] synthesized $Ca_xCu_{3-x}Ti_4O_{12}$ (x = 1.0, 1.5 and 2.0) nanopowders using the organic acid precursor method; the samples were annealed at 1000 °C for 2 h. They found that E_g increased from 3.12 to 3.26 eV, respectively, with increasing molar ratio. Pandey et al. [1] observed that the E_g about 3.4 eV for CCTO pellets prepared at 400 °C was about 3.4 eV. Ning et al. [23] coated a CCTO thin film on $LaAlO_3$ substrates at 820 °C by using pulse laser deposition (PLD) and found the E_g to be about 2.88 ev. The increase in grain size weakened the quantum size effects thus leading to the decrease in E_g value [24]. Quantum size effects become important when the grain size becomes smaller (D < 100 nm). In this case, grains behave as quantum wells and the energy band gap is associated with grain size [24]. The energy band gap's variation with rain size due to quantum confinement can be expressed in quantitative form (Eq. 4) [25]:

$$E_g = \frac{h^2\pi^2n^2}{2mr^2} \tag{4}$$

where E_g is energy band gap, r is the radius of the grain, m the effective mass of the system and h is planck's constant. According to Eq. 2, the E_g has an inverse relationship with grain size. Therefore, it is believed that an increase in annealing temperature causes a decrease in E_g. In conclusion, the results of this study suggest that 200 nm thick CCTO thin films can potentially be used for applications in nonlinear optical devices. The data evaluated from the XRD, FESEM, EDAX, AFM, and UV–Vis measurements of CCTO thin films after annealing at different temperatures are shown in Table 2.

The resistance behavior of CCTO thin films according to annealing temperature is shown in Fig. 6. With the increase in annealing temperature, the resistance of thin

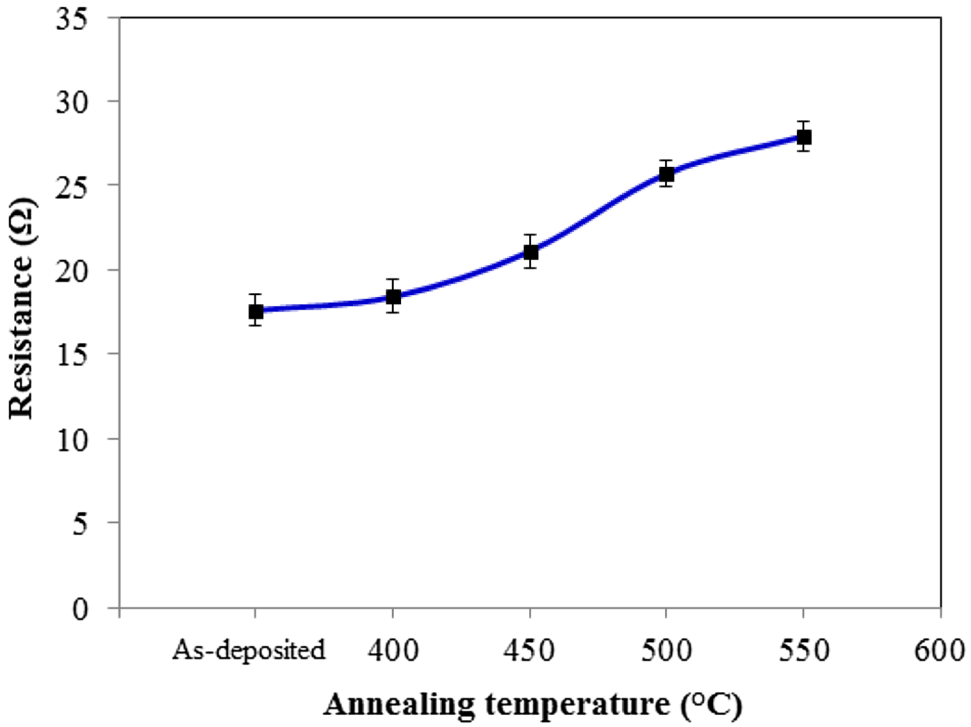

Fig. 6 Resistance of CCTO thin films as a function of annealing temperature. Data measured at relative humidity of 30% and 3 V

films increases. The highest resistance value for CCTO thin film was obtained at 550 °C annealing temperature. The resistance of thin films depends on its crystalline state [26]. At an annealing temperature of 550 °C, the XRD diffraction peak intensity was strongest with good crystalline quality due to increases in grain size [27]. Increases in the annealing temperature attributed to increase in grain size. Increases in grain size accompanied by a reduction in the actual number of grains per volume led to a decrease in grain boundary. Grain boundaries are 2D defects in the crystal structure and tend to decrease the electrical of the material. Grain boundaries with large amounts of defects will block the carrier transition; this results in an increase in resistivity.

4 Conclusion

CCTO thin films with a thickness of 200 nm were deposited on ITO substrate by RF magnetron sputtering. The effects of annealing temperature on structural and optical properties and surface morphology of CCTO thin films were investigated. The results show that the crystallinity, grain size, and surface roughness of as-deposited CCTO thin films increased with annealing temperature. In addition, the optical transmittance and E_g values decreased with increase in annealing temperature; this can be explained in terms of the quantum-size effect. The CCTO thin films annealed at 550 °C had high resistivity. Therefore, it can be concluded that the desirable crystallinity, surface roughness, and E_g properties for the 200 nm CCTO thin films deposited by RF magnetron sputtering can be achieved through the annealing process.

Acknowledgements This research was supported by the Universiti Sains Malaysia (USM) fellowship (APEX 91002/JHEA/ATSG4001) and fundamental research grant scheme (FRGS) under grant number of 203/PBAHAN/6071263.

References

1. R.K. Pandey, W.A. Stapleton, J. Tate, A.K. Bandyopadhyay, I. Sutanto, S. Sprissler, S. Lin, AIP Adv. **3**(6), 062126 (2013)
2. J.P. Gonjal, R. Schmidt, E. Morán, Microwave-assisted synthesis and characterization of perovskite oxides, perovskite: crystallography, chemistry and catalytic performance, Chap 4. (Novascience Publishers, Hauppauge, 2013), pp. 117–140, ISBN: 978-1-62417-800-9
3. M. Ahmadipour, M.F. Ain, Z.A. Ahmad, Appl. Surf. Sci. **385**, 182–190 (2016)
4. R. Lohnert, H. Bartsch, R. Schmidt, B. Capraro, J. Topfer, J. Am. Ceram. Soc. **98**(1), 141–147 (2015)
5. M. Li, X.L. Chen, D.F. Zhang, W.Y. Wang, W.J. Wang, Sens. Actuat. B. **147**(2), 447–452 (2010)
6. L.C. Kretly, A.F.L. Almeida, R.S. de Oliveira, J.M. Sasaki, A.S.B. Sombra, Microw. Opt. Technol. Lett. **39**(2)145–150 (2003)
7. E. Joanni, R. Savu, P.R. Bueno, E. Longo, J.A. Varela, Appl. Phys. Lett. **92**(13), 132110–132113 (2008)
8. S.F. Shao, J.L. Zhang, P. Zheng, W.L. Zhong, C.L. Wang, J. Appl. Phys. **99**(8), 084106–084111 (2006)

9. L. Laijun, F. Huiqing, F. Pinyang, C. Xiuli, Mater. Res. Bull. **43**(7), 1800–1807 (2008)
10. L. Fang, M.R. Shen, Thin Solid Films **440**(1–2), 60–65 (2003)
11. P. Fiorenza, R. Lo Nigro, A. Sciuto, P. Delugas, V. Raineri, R.G. Toro, M.R. Catalano, G. Malandrino, J. Appl. Phys. **105**(6)061634 (2009)
12. M. Ahmadipour, M.F. Ain, Z.A. Ahmad, Nano Micro Lett. **8**(4)291–311 (2016)
13. B.S. Prakash, K.B.R. Varma, D. Michau, M. Maglione, Thin Solid Films **516**(10), 2874–2880 (2008)
14. M. Ahmadipour, M.J. Abu, M.F.A. Rahman, M.F. Ain, Z.A. Ahmad, Micro-Nano Lett. **11**(3)147–150 (2016)
15. N. Terinte, R. Ibbett, K. C. Schuster, Lenzinger Ber. **89**, 118 (2011)
16. M. Ahmadipour, M.F. Ain, Z.A. Ahmad, Measurement **94**, 902–908 (2016)
17. Y.W. Phuan, M.N. Chong, T. Zhu, S.T. Yong, E.S. Chan, Mater. Res. Bull. **69**, 71–77 (2015)
18. L. Fang, M. Shen, J. Appl. Phys. **95**(11), 6483–6485 (2004)
19. S.H. Kang, Y.S. Obeng, M.A. Decker, M. Oh, S.M. Merchant, S.K. Karthikeyan, C.S. Seet, A.S. Oates, J. Electron. Mater. **30**(12), 1506–1512 (2001)
20. S. Chander, M.S. Dhaka, Phys. E **80**, 62–68 (2016)
21. E.S.M. Goh, T.P. Chen, C.Q. Sun, Y.C. Liu, J. Appl. Phys. **107**(2), 024305–024305 (2010)
22. A.O. Turky, M.M. Rashad, Z.I. Zaki, RSC Adv. **5**, 18767–18772 (2015)
23. T. Ning, C. Chen, Y. Zhou, H. Lu, D. Zhang, H. Ming, G. Yang, Appl. Phys. A. **94**(3) 567–570 (2009)
24. M. Ohtsu, Nanophotonics and nanofabrication. (Wiley, New York, 2015)
25. L.E. Brus, J. Chem, Phys. **80**(9)4403–4409 (1984)
26. H.F. Zhang, H. Liu, L. Feng, Vacuum **84**(6)833–836 (2010)
27. Y.S. Shen, B.S. Chiou, C.C. Ho, Thin Solid Films **517**(3), 1209–1213 (2008)